Journal of Cleaner Production 274 (2020) 122941

Contents lists available at ScienceDirect

Journal of Cleaner Production

journal homepage: www.elsevier.com/locate/jclepro

The mitigation strategy of automobile generated fine particle pollutants by applying vegetation configuration in a street-canyon

Lu Zhang [a], Zhiqiang Zhang [a, *], Steven McNulty [b], Ping Wang [a]

[a] Key Lab of Soil & Water Conservation and Desertification Combating, College of Soil and Water Conservation, Beijing Forestry University, Qinghua East Road 35, Haidian District, Beijing, 100083, PR China
[b] USDA Southeast Regional Climate Hub, 920 Main Campus, Dr. Venture Center 2, Suite 300, Raleigh, NC, 27606, USA

ARTICLE INFO

Article history:
Received 26 April 2020
Received in revised form
3 June 2020
Accepted 17 June 2020
Available online 17 July 2020

Handling editor. M.T. Moreira

Keywords:
Street-canyon
Vegetation effect
Vegetation configuration
Pollutant dispersion
Pollutant deposition
CFD

ABSTRACT

Urban vegetations are widely used as one of the mitigation approaches to combat the public health threat from air particulate matter (PM) pollution for urban residents. However, vegetation effect at the points of interest (e.g. leeward wall, windward wall, pedestrian-level) in street-canyon from different vegetation configurations on the air quality is still not well established. We, therefore, used the numerical simulation approach to evaluate vegetation effect (VE) for different vegetation configurations (VCs) (e.g. tree or tree-shrub plantings in two sides and either side of windward or leeward) with several tree species on the traffic-originated PM pollutants in a street-canyon under a perpendicular wind. The total VE varied from −4.0% to 20.6% while pedestrian-level VE from −3.5% to 15.4% depending on different VCs. Cypress species have better total VE varying from 3.5% to 11.5% and pedestrian-level VE from 4.8% to 10.9% than the other species for same VC due to its higher deposition velocity. For those only trees used cases, the best VEs (pedestrian-level VE: 3.3%–10.9%; total VE: 2.1%–11.5%) were found on the leeward side planting where is closer to the higher polluted domain and had less obstructions for wind movement. We found that two sides planting of enhanced tree-shrub configuration by Cypress in the street-canyon was an optimal strategy to improve the total VE by 19.3%–20.6% and pedestrian-level VE 14.1%–15.4%, as well as mitigate the highly concentrated PM in the street center. The VE for the leeward wall was significantly correlated with aerodynamic parameter ($C_d LAD$) ($P < 0.001$) while VEs for the windward wall and pedestrian level with deposition parameter ($LADv_d$) ($P < 0.001$). Clearly, street-canyon air quality can be improved by making good use of pressure loss coefficient of vegetation to alter pollutants distribution and selecting vegetation with high deposition velocity to filter more pollutants. Our research provides insights for urban planners and designers to develop the best management practices of urban forestry.

1. Introduction

Air quality in the built environment is a primary concern for people living in urban areas (Wu et al., 2018). Road traffic emits a variety of harmful pollutants in the form of particulate matter (PM10, PM2.5, and UFP) (Abhijith et al., 2017) and gaseous chemical pollutants (NOx, SOx, CO, and O_3) (Haakman et al., 2020). The gaseous pollutants may also form secondary particles that are generally smaller than 2.5 μm using nucleation, condensation, or coagulation (Dzierżanowski et al., 2011). Thus, road traffic-originated emissions commonly constitute the primary source for atmospheric particulate pollution in urban streets (Gromke and Ruck, 2012) and have multiple adverse health effects on urban residents (Song et al., 2016). Urban structures with streets and buildings of different sizes and shapes have complex wind patterns. Street-canyon as the typical architectural structure can be heavily polluted regions within a city because of the reduced air exchange, vortices formed by wind flow, and the subsequent recirculation of traffic-generated pollution between surrounding buildings (Jeanjean et al., 2015).

Given the high levels of pollutant exposure for pedestrians and residents in roadside buildings, it is therefore of great importance to adopt appropriate measures to mitigate traffic-induced air pollution in street-canyons (Xue and Li, 2017). Vegetation planting

* Corresponding author.
E-mail address: zhqzhang@bjfu.edu.cn (Z. Zhang).

https://doi.org/10.1016/j.jclepro.2020.122941

is one of the most popular means for improving the outdoor and indoor environment (Mochida et al., 2008). Several field studies have shown that vegetation can significantly alter the pollutant distribution within street-canyons (Al-Dabbous and Kumar, 2014). Specifically, trees have the potential to affect local air quality mainly in two ways (Xue and Li, 2017): aerodynamic effect (Gromke et al., 2016) and deposition effect (Litschke and Kuttler, 2008). In terms of aerodynamic effect, vegetation obstructs the airflow and decreases air ventilation (Xue and Li, 2017). Denser tree crowns can lower the flow velocity (Hofman et al., 2016), reduce the air exchange with the surroundings at the canyon roof and ends (Gromke, 2011), thus produce a higher pollutant concentration (Gromke and Ruck, 2012), which are confirmed by wind tunnel experiments and numerical simulations. However, these studies have only considered the impact of plants on the flow field and have failed to take deposition effect into account, which may lead to overestimation in pollution level (Xue and Li, 2017). Plants have the capability of filtering out particulate matters from the atmosphere (Beckett et al., 2000; Terzaghi et al., 2013) by deposition onto leaf surfaces (Mitchell et al., 2010). Full-scale field measurements showed that trees could accumulate pollutants (Salmond et al., 2013) and tree canopy density, leaf area index, and air velocity are the most effective factors affecting the attenuation coefficient of PM2.5 in street-canyons (Jin et al., 2014).

In-situ field measurements, wind tunnel tests, as well as the CFD simulations failed to reach a consensus on whether or not the roadside trees/vegetation universally mitigate air quality in the street-canyon (Abhijith et al., 2017). These inconclusive findings suggest that it is necessary to explore the local vegetation effects under different scenarios as impacted by multiple interacting factors (Buccolieri et al., 2018). For instance, the impact of the same roadside vegetation may vary under different wind directions in the street-canyon: most effective reduction in pollutant concentration under parallel wind direction; trapping more pollutants to increase the pollution concentration under perpendicular wind direction (Buccolieri et al., 2018). Understanding how to alleviate the heavily polluted region in a street-canyon by vegetation is essential for developing sound tree planting practices. However, most of the previous studies have only evaluated the effect of a single factor such as wind direction (Di Sabatino et al., 2008; Kumar et al., 2008), the street-canyon aspect ratio (Gromke, 2013; Gromke and Ruck, 2012), or the aerodynamic effect (Buccolieri et al., 2009; Gromke et al., 2016) or/and deposition effect (Hong et al., 2017; Xue and Li, 2017) of vegetation on pollutant concentration in a street-canyon. The impact of different vegetation configurations and tree species have not been explored and documented even though such information is vital for developing best management practices in urban forestry. Also, there are limited opportunities for increasing tree density within a street-canyon environment due to space constraints (Salmond et al., 2013). Intensive labor and resources consumption for in-situ measurements of air pollutants, the numerical simulation approach using the CFD have been widely used to investigate the urban pollutant transportation, movement, and deposition under different boundary and initial conditions with the goal of providing an urban design reference for urban air quality management (Toparlar et al., 2017).

We, therefore, used a numerical simulation approach to evaluate vegetation effect (VE) for vegetation configurations (VCs) with several tree species on the dispersion, deposition, and distribution of traffic-originated fine particulate pollutants in a street-canyon under perpendicular wind direction. Our study objectives were to: (1) quantify the difference in the VEs between different VCs with several tree species (i.e., *Populus*, *Pinus* and *Cupress*); (2) evaluate the VE inside a street-canyon from multiple perspectives; (3) explore the governing mechanism of vegetation parameters on the VE, and (4) elucidate an optimal VC strategy using a series of simulations and comparisons. Our research provides insights for urban planners and designers to develop the best management practices of urban forestry for maximizing the air purification capability of roadside vegetation.

2. Methodology

2.1. Scenario descriptions

A generic urban street-canyon of 180m length (L), 36m width (W) and 18m height (H) (i.e., the street aspect ratios W/H = 2 and L/H = 10) formed by two parallel aligned buildings of 180 m × 18 m × 18m (L × H × H) with a distance of 36m (2H) was investigated (Fig. 1A). Previous results showed that the tree canopy space has little effect on pollutant concentrations under the perpendicular wind (Buccolieri et al., 2011). Therefore, avenue-like design of planted mature trees and shrubs extending over the entire street length with neighboring canopies was used for our study (Gromke and Ruck, 2009). Various scenarios for VCs are provided in Fig. 1B and C. Only vegetation canopies were modeled while trunks were not (Xue and Li, 2017), because their volume is quite small compared with the canopies and has little impact on the flow (Yang et al., 2020). Road vegetation were parameterized in the four following arrangements: (I) trees planted on two sides of the street (Fig. 1B (b) and 1C (i)), (II) trees planted on the windward side of the street (Fig. 1B (c) and 1C (i)) or the leeward side of the street (Fig. 1B (d) and 1C (i)), (III) tree-shrub configurations (Fig. 1B (e) (f) and 1C (j)) and (IV) enhanced tree-shrub configurations (Fig. 1B (g) (h) and 1C (k) (l)).

To evaluate the influence of different vegetation species on pollutant concentration, the establishment of specific parameters to describe vegetation is important. Three typical tree species Pine (*Pinus*), Cypress (*Cupress*), and Poplar (*Populus*) were selected, as the three tree species have a significant difference in dry deposition velocities (v_d) (Freer-smith et al., 2005). A drag coefficient (C_d) is dependent on the species and for most vegetations ranging from 0.1 to 0.3 (Katul et al., 2004). In this study, we set $C_d = 0.2$ for Poplar to reflect an average value (Gromke and Blocken, 2015) and $C_d = 0.25$ for Pine and Cypress because the drag coefficient of Poplar canopy is smaller than that of conifers (Koizumi et al., 2010). Leaf area density (*LAD*, total leaf area divided by the total volume of vegetation, $m^2\ m^{-3}$) is another significant parameter for assessing vegetation effects (Vos et al., 2013), and we designated three levels of *LAD* of 0.5, 1, 2 for trees. As hedges were generally denser than trees, we have set 4 $m^2\ m^{-3}$ for shrub *LAD* (Vos et al., 2013). Dry deposition velocities are highly related to the vegetation species and particle diameters (Jeanjean et al., 2016). For outdoor air pollution, fine particulate matter poses the greatest threat to human health (Lelieveld et al., 2015). Therefore, we focused on fine particulate matter PM2 in our study. Overall, 20 study cases, 3 validation cases, and 1 reference case were set up (Table 1).

2.2. CFD model

Three-dimensional steady-state simulations were performed to study the vegetation impact on air quality in a street-canyon via the ANSYS Fluent software (ANSYS, Inc., PA, U.S.A.). The computational domain and grid were generated by ICEM CFD (ANSYS, Inc., PA, U.S.A.).

2.2.1. Computational domain and boundary conditions

The computational domain (Xue and Li, 2017) and boundary conditions (Gromke et al., 2008) (Fig. 2) were made by the recommendations. For the inlet boundary (Buccolieri et al., 2009), a

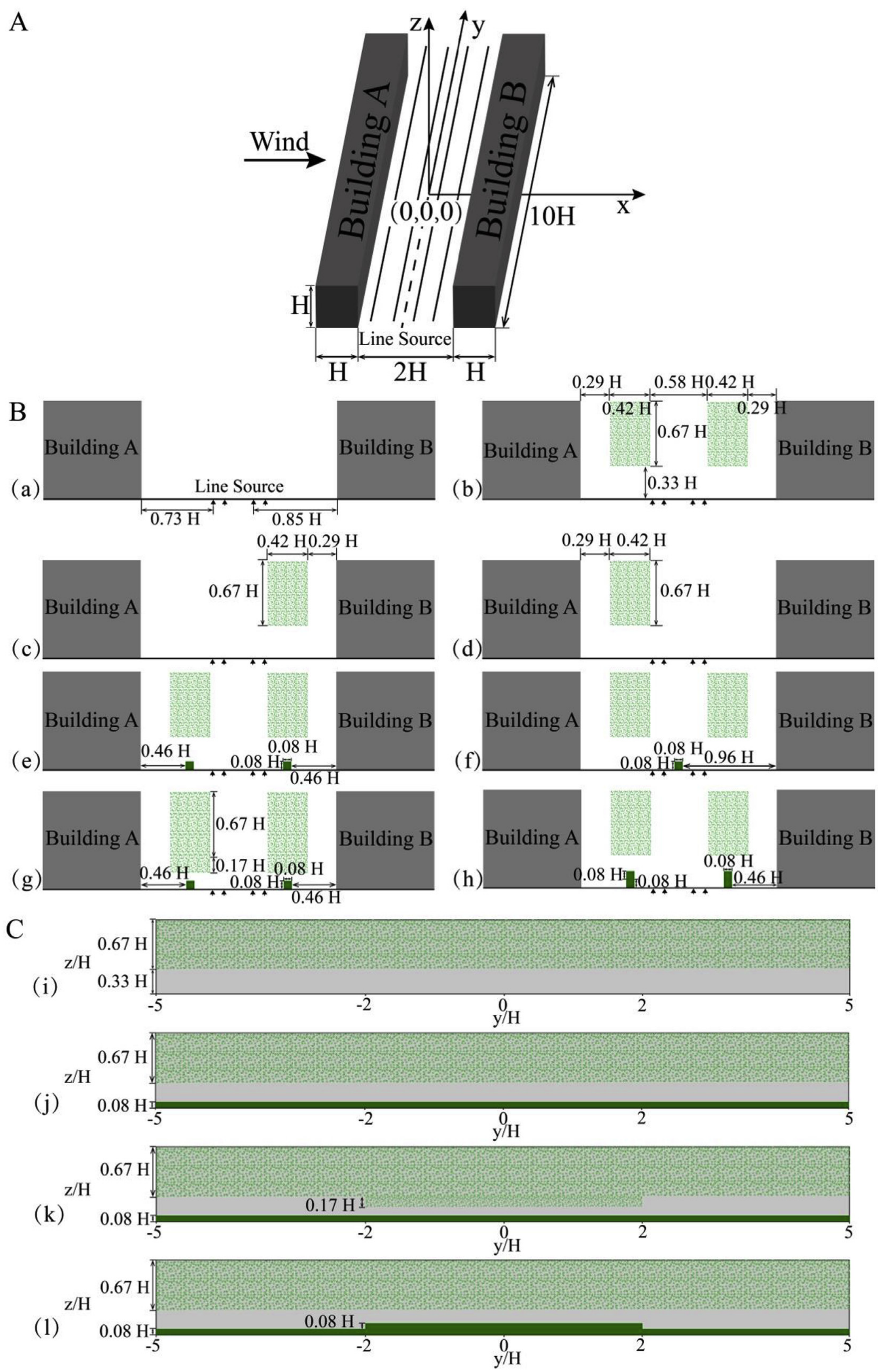

Fig. 1. Investigated scenarios: (A) street-canyon model size, (B) Cross-sectional view of VC; (C) Longitudinal view of VC.

Table 1
Investigated cases set up with different VCs.

VC	Case Name	VC description	Leaf area density (m^2 m^{-3})	Drag coefficient	PM2 deposition velocity (m s^{-1})	Schematic diagram Fig. 1B and C
Two sides planting	$C_{Pine\text{-}Pine}$	Pine on two sides	0.5,1,2	0.25	0.018	(b) & (i)
	$C_{Cypress\text{-}Cypress}$	Cypress on two sides	0.5,1,2	0.25	0.046	
	$C_{Poplar\text{-}Poplar}$	Poplar on two sides	0.5,1,2	0.2	0.008	
Leeward side planting	$C_{Pine\text{-}0}$	Pine on the leeward side	2	0.25	0.018	(d) & (i)
	$C_{Cypress\text{-}0}$	Cypress on the leeward side	2	0.25	0.046	
	$C_{Poplar\text{-}0}$	Poplar on the leeward side	2	0.2	0.008	
Windward side planting	$C_{0\text{-}Pine}$	Pine on the windward side	2	0.25	0.018	(c) & (i)
	$C_{0\text{-}Cypress}$	Cypress on the windward side	2	0.25	0.046	
	$C_{0\text{-}Poplar}$	Poplar on the windward side	2	0.2	0.008	
Tree-Shrub configuration	$C_{Tree\text{-}Shrub1}$	Cypress-Shrub on two sides	2–4	0.25–0.3	0.046–0.02	(e) & (j)
	$C_{Tree\text{-}Shrub2}$	Cypress-Shrub on two sides	2–4	0.25–0.3	0.046–0.05	(e) & (j)
	$C_{Tree\text{-}Shrub\text{-}Tree}$	Cypress on two sides and Shrub on the longitudinal street axis	2-4-2	0.25–0.3-0.25	0.046–0.05-0.046	(f) & (j)
Enhanced Tree-Shrub configuration	$C_{Tree\ down\text{-}Shrub}$	Cypress-Shrub on two sides with the central part of Cypress canopy (y/H from-2 to 2) vertically extending down by 0.17H	2–4	0.25–0.3	0.046–0.05	(g) & (k)
	$C_{Tree\text{-}Shrub\ up}$	Cypress-Shrub on two sides with the central part of Shrub (y/H from-2 to 2) vertically extending up by 0.08H	2–4	0.25–0.3	0.046–0.05	(h) & (l)
Reference	$C_{Reference}$	Treeless	0	0	0	(a)
Validation	$C_{Validation1}$	Treeless	0	0	0	(a)
	$C_{Validation2}$	Trees on two sides	2	0.265	0	(b) & (i)
	$C_{Validation3}$	Trees on two sides	4	0.3325	0	(b) & (i)

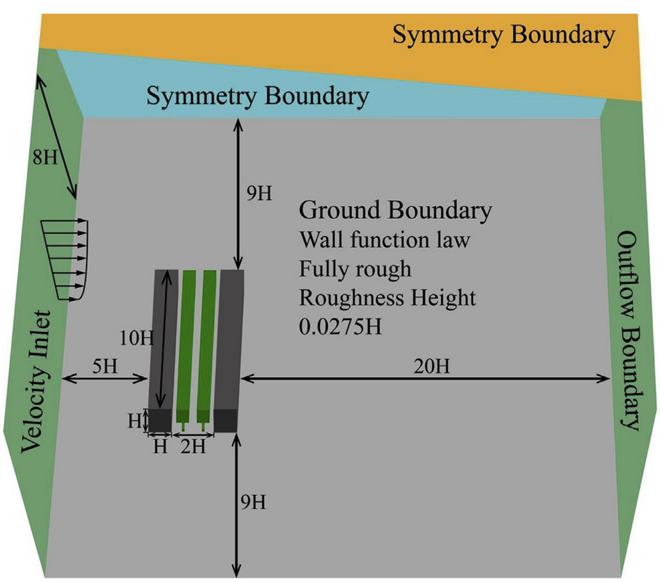

Fig. 2. Bird's eye view of the computational domain and boundary conditions.

power-law profile for mean velocity (Eq. (1)), turbulent kinetic energy, k (m^2 s^{-2}) (Eq. (2)), and turbulence dissipation rate ε (m^2 s^{-3}) (Eq. (3)) for a neutrally stratified atmospheric boundary layer (Gromke et al., 2008) were adopted:

$$u(z) = u_H(z/H)^{\alpha} \tag{1}$$

where u(z) is the wind speed at height z, $u_H = 4.70$ m s^{-1} is the mean velocity at height H and an empirical constant $\alpha = 0.30$ in the wind tunnel experiment was used as reference (Buccolieri et al., 2009).

$$k = \left(u_*^2 \Big/ \sqrt{C_\mu}\right)(1 - z / \delta) \tag{2}$$

$$\varepsilon = \left(u_*^3 \Big/ (\kappa z)\right)(1 - z / \delta) \tag{3}$$

Where $u_* = 0.52$ m s^{-1} is the friction velocity, δ is the boundary layer depth (m), $C_\mu = 0.09$ is a coefficient used to define the eddy viscosity in turbulence models and $\kappa = 0.4$ is the von Kàrmàn constant.

2.2.2. Airflow model

Reynolds-Averaged Navier-Stokes (RANS) equations were solved with the Reynolds stress turbulent model (RSM) (Buccolieri et al., 2009; Endalew et al., 2009). RSM model has better performance in predicting flow field and complex dispersion process than the k-ε model (Gromke et al., 2008). The SIMPLE scheme was used for the pressure-velocity coupling, and the discretization schemes were set second-order upwind (Liu et al., 2017).

2.2.3. Vegetation model

Vegetation was represented by setting porous fluid zones that were assigned to additional terms in the governing equations (Qin et al., 2019; Xue and Li, 2017) to model its aerodynamic and deposition impact. The momentum loss S_m was added to the momentum equation as the sink term to model the aerodynamic effect, by adding a pressure loss coefficient to the vegetation zone to account for the inertial resistance induced by the vegetation (Jeanjean et al., 2017). The momentum sink term of vegetation canopy was modeled as follows:

$$S_m = -(1 / 2)\rho C_d LADUu_i \tag{4}$$

where S_m is the momentum loss by vegetation (kg m^{-2} s^{-2}); ρ is the air density (kg m^{-3}); U is the local mean wind speed (m s^{-1}), u_i is the $i-th$ direction wind speed, (m s^{-1}), and C_dLAD is defined the pressure loss coefficient (m^{-1}).

Changes of turbulence kinetic energy (S_k, Eq. (5)) and turbulence dissipation rate (ε_k, Eq. (6)) were added to the transport equation as the source terms of k and ε, respectively (Mochida et al., 2008), to represent the turbulence due to branches and leaves. The source terms were given by (Sanz, 2003):

$$S_k = \rho C_d LAD\left(\beta_p U^3 - \beta_d Uk\right) \tag{5}$$

$$\varepsilon_k = \rho C_d LAD(\varepsilon / k)\left(C_{\varepsilon 4}\beta_p U^3 - C_{\varepsilon 5}\beta_d Uk\right) \tag{6}$$

where the constants $\beta_p = 1.0$, $\beta_d = 3.0$ (Katul et al., 2004) and $C_{\varepsilon 4} = C_{\varepsilon 5} = 1.5$ (Sanz, 2003) were adopted.

2.2.4. Traffic emissions simulation

The line sources were simulated by separating four volume at street ground-level in the geometry and defining the four volumes as separate fluid zones for emitting pollutant (Salim et al., 2011). The line sources exceed the street-canyon by 0.92H on each side to simulate the traffic emission of the intersections (Fig. 4). The emission rate of each line Q was set at 0.01 kg s^{-1} of PM2 for investigated cases and of Sulfur hexafluoride (SF6) used in wind tunnel experiments for validation cases.

2.2.5. Dispersion modeling

For pollutant dispersion, the advection-diffusion equation was used (Gousseau et al., 2011; Gromke et al., 2008). In turbulent flows, ANSYS Fluent predicts the mass diffusion according to:

$$J = -(\rho_m D + \mu_t / Sc_t)\nabla Y \tag{7}$$

where D is the molecular diffusion coefficient for the pollutant in the mixture, μ_t is the turbulent viscosity, Y is the mass fraction of the pollutant, and ρ_m is the mixture density. The turbulent viscosity is computed as $\mu_t = \rho_m(C_\mu k^2 / \varepsilon)$. The turbulent Schmidt number is computed as $S_{Ct} = \mu_t/(\rho_m D_t)$, where D_t is the turbulent diffusivity. S_{Ct} is an important parameter in diffusion simulation. Previous studies have reported a series values of S_{Ct}, such as 0.2–1 (Gromke et al., 2008), 0.5 (Gromke and Blocken, 2015; Jeanjean et al., 2015), 0.7 (Salim et al., 2011) and 1 (Vranckx et al., 2015; Xue and Li, 2017) for different research cases based on different turbulent models. S_{Ct} depends strongly on the flow topology and source characteristic (Blocken et al., 2008). In this study, the S_{Ct} has been optimized to be 1.0 according to the comparison with wind tunnel data (Gromke, 2013), which is consistent with the same numerical and experimental scenarios (W/H = 2) investigated by previous works (Vranckx et al., 2015; Xue and Li, 2017).

2.2.6. Vegetation effect on the particle concentration

The deposition effect of vegetation on the particulate matter was modeled as an additional sink term and added in the conservation equation below:

$$\nabla \cdot (\rho u Y) = \nabla \cdot [(\rho_m D + \mu_t / Sc_t)\nabla Y] + S_{deposition} \tag{8}$$

$S_{deposition}$ is the mass of particles deposited by vegetation per cubic meter (kg m^{-3}). The deposition effect of vegetation modeled by a concentration source term as follows (Ji and Zhao, 2014; Xue and Li, 2017),

$$S_{deposition} = -LAD v_d C \tag{9}$$

where C is the local concentration (kg m^{-3}), defined by $C = Y \cdot \rho_m$.

2.2.7. Normalized simulated concentration

The simulated concentration data were normalized as previous literature (Gromke, 2013) to facilitate validation and comparison according to:

$$C^+ = C_m u_H H / (Q_T / L) \tag{10}$$

where C_m is the simulated concentration, C^+ is the normalized concentration and Q_T/L is the emission rate per unit length of the source (kg m^{-1} s^{-1}).

2.2.8. Vegetation effect (VE)

(1) Quantified vegetation effect (VE)

Vegetation effect (VE) was evaluated by relative change rate (%), which was calculated as the deviation in area-averaged normalized PM concentration per investigated area between each case with vegetation and the reference case according to the following equation:

$$VE\ (\%) = \left(C_{Reference} - C_{Vegetation}\right) \Big/ C_{Reference} \times 100\% \tag{11}$$

A positive VE (+ %) means that vegetation could decrease the PM concentration (e.g., beneficial effect), while the negative VE (- %) means that vegetation could increase the PM concentration (e.g., deteriorative effect).

(2) VEs on investigated areas

The VE inside street-canyon was evaluated from multiple perspectives of each VC: leeward and windward, representing the investigated area that outdoor vehicular particles easily penetrate indoors via doors/windows (Chen et al., 2012; Ji and Zhao, 2015), ventilation systems and building cracks etc (Yang et al., 2020); pedestrian level, representing the investigated area that gives high level of pollutant exposure for pedestrians; the total VE: evaluate the overall effect of each VC.

From Fig. 3, the VEs of the leeward wall and windward wall were evaluated by the paralleled planes at 0.75m away from building A and building B inside the street-canyon; the VE of the pedestrian level was evaluated by the horizontal plane at mean breathing height (1.5m) inside the street-canyon; the total VE was evaluated by the sum of area-averaged normalized PM concentration of leeward wall, windward wall, and pedestrian level in each VC.

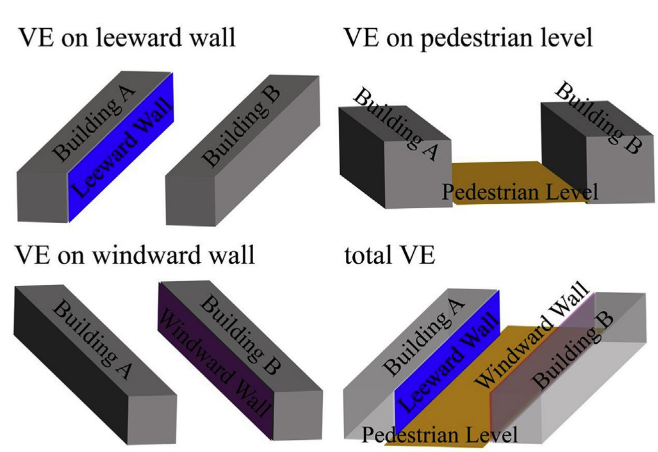

Fig. 3. VEs on investigated areas.

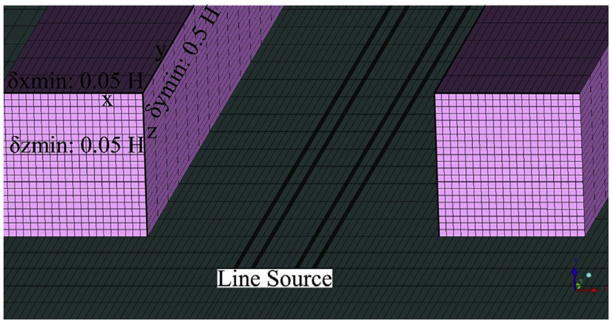

Fig. 4. Computation grids.

2.3. Grid insensitive solutions and model validation

The numerical model was validated against the wind tunnel database (http://www.codasc.de) provided by CODASC. The wind tunnel data and simulation data were analyzed using MATLAB software (MathWorks Inc.).

2.3.1. Grid insensitive solutions

A grid sensitivity study indicated that a cell count of 20 per building height and 12 per canyon width is sufficient for reasonable grid insensitive solutions (Gromke and Blocken, 2015). The hexahedral cell counts in this CFD study meeting the requirements (Fig. 4). In addition, we compared normalized concentration distribution of the treeless case by medium and fine grid resolutions and there is of little difference (result was not presented), so the medium grid is adopted to save computation time. The final number of the structured grids used for all simulations was approximately 750,000 (Buccolieri et al., 2009).

2.3.2. Model validation

The pollutants distribution pattern was well reproduced by simulations and the relative difference was within 20% in most positions, especially for leeward wall (Fig. 5 a1, b1, c1), although relative deviations were as much as 40% in some position of windward wall (Fig. 5 a2, b2, c2) due to small absolute values of pollutant concentration. The largest relative deviations were at street ends due to lower pollutant concentrations.

Statistical analysis was conducted according to the instruction (Hanna and Chang, 2012) to evaluate the overall model performance. Several recommended metrics were adopted, including the average concentration, the fractional bias (FB), the normalized mean square error (NMSE), the fraction of predictions within a factor of two of observations (FAC2) and the relation coefficient (R). Hanna and Chang (2012) recommended a set of acceptance criteria: $-0.3 < FB < 0.3$, $NMSE < 1.5$, $FAC2 > 0.5$, $R > 0.8$. In Table 2, all metrics are within acceptable criteria. Overall, the validation shows that the numerical model is suitable for predicting the airflow and pollutant dispersion within the street-canyon.

3. Results

3.1. VEs for different VCs

For the reference case (i.e., $C_{Reference}$, Treeless), the normalized PM concentration distribution pattern was in Fig. 6$C_{Reference}$. PM concentration of the leeward wall was larger than that of the windward wall in the treeless street-canyon. PM concentration on the windward wall, leeward wall, and pedestrian level were all decreased from the street center to the street ends. The following sections are compared with the Reference case.

3.1.1. VEs by two sides planting

Two sides planting led to the higher PM concentration near the leeward wall and a lower PM concentration near windward compared with that of the reference case (Fig. 6, Trees on both side panel). The VEs by two sides planting were in Fig. 7A. Leeward wall VE was negative and decreased with *LAD* increase, while windward wall VE was positive and increased with *LAD* increase for the same tree species. Pedestrian-level VE was positive and increased with *LAD* for Cypress and Pine, however, pedestrian-level VE of Poplar was positive only for $LAD = 2$. For the same *LAD*, the windward wall VE and the pedestrian-level VE of the Cypress were maximum and of Poplar were minimum. Collectively, the maximum positive VE was achieved by Cypress with $LAD = 2$.

3.1.2. VEs by one side planting

The patterns of particle distribution were similar to the two sides planting (Fig. 6 Trees on the windward side and Trees on leeward side panels). The VEs by one side planting were in Fig. 7B. The VEs of pedestrian level and windward wall were remained positive and the leeward wall VE were remained negative by one side planting. Across the three species, Cypress had the best VE. For the same tree species, pedestrian-level VE and leeward wall VE by the leeward side planting were better than those by the windward side planting. Compared to different sides planting, negative leeward wall VE for leeward side planting was least.

3.1.3. VEs by tree-shrub configurations

In the above, the Cypress had a better VE than the other tree

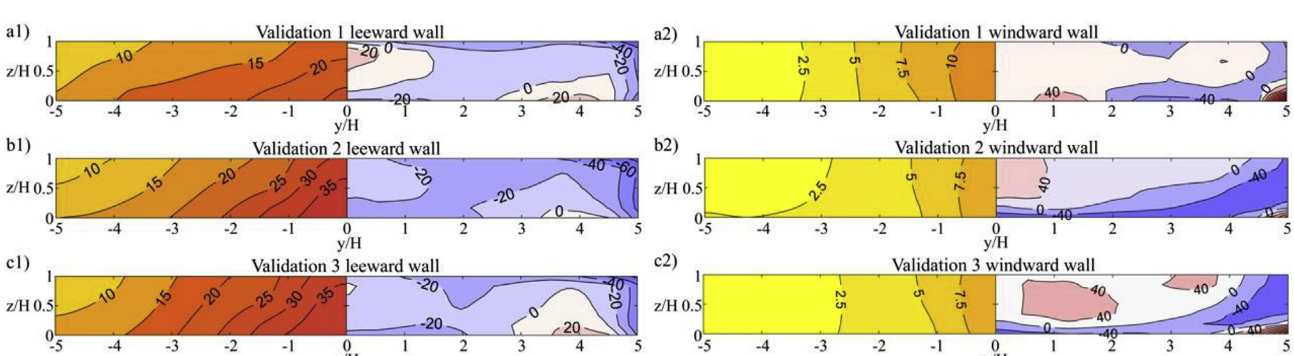

Fig. 5. Normalized concentration distribution of wind tunnel (the right of each panel) and the relative difference of simulated data (the left of each panel) near leeward wall and windward wall of three validation cases.

Table 2
Statistical analysis for overall model performance.

Validation cases	Wall	Mean normalized concentration			Statistical analysis metrics			
		Wind tunnel	Numerical simulation	Relative difference (%)	FB	NMSE	FAC2	R
$C_{Validation1}$	Leeward	14.96	14.07	−5.97	0.062	0.033	1	0.894
	Windward	5.14	6.15	19.85	−0.181	0.118	0.986	0.977
$C_{Validation2}$	Leeward	20.76	16.02	−22.81	0.258	0.090	1	0.944
	Windward	3.83	4.05	5.79	−0.056	0.222	0.991	0.886
$C_{Validation3}$	Leeward	20.89	18.10	−13.36	0.143	0.045	1	0.945
	Windward	3.46	4.18	20.64	−0.187	0.206	0.983	0.906

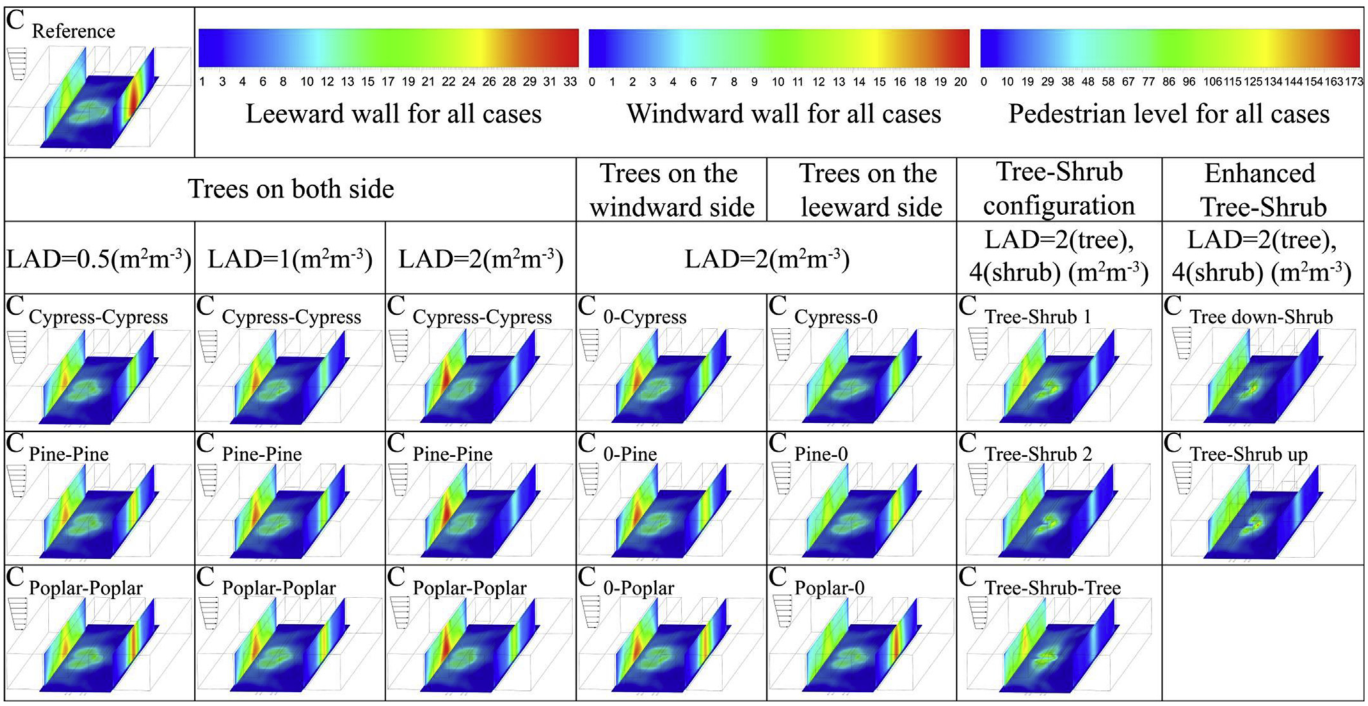

Fig. 6. Distribution of simulated PM concentration near the leeward wall, windward wall, pedestrian level for all cases.

species. Therefore, Cypress and Shrub were arranged for Tree-Shrub configuration to see if the VE could be further increased. We evaluated the different deposition velocity of Shrub in Tree-Shrub configurations to find out if there are different VEs for the same VC. The patterns of particle distribution were similar to the only Tree used cases (Fig. 6 Tree-Shrub configuration panel and Enhanced Tree-Shrub configuration panel). The VEs by Tree-Shrub configurations were in Fig. 7C. The VE of Cypress-Shrub on two sides with a higher v_d for Shrub ($C_{Tree\text{-}Shrub\ 2}$) was better than that of $C_{Tree\text{-}Shrub\ 1}$ with a lower v_d. The pedestrian-level VE for Cypress-Shrub on two sides ($C_{Tree\text{-}Shrub\ 2}$) was better than Cypress on two sides and Shrub on the street axis ($C_{Tree\text{-}Shrub\text{-}Tree}$) with the same v_d. The VEs by two enhanced cases ($C_{Tree\ down\text{-}Shrub}$ and $C_{Tree\text{-}Shrub\ up}$) were better than the other Tree-Shrub configuration cases, and their VEs on leeward wall were less than −8.5%, which was the least of all simulated cases. The higher concentration on the central area of both the leeward and windward walls was mitigated by the two enhanced Tree-Shrub cases (Fig. 6). Overall, the VE of $C_{Tree\ down\text{-}Shrub}$ was best of all.

3.2. VEs comparison for all VCs

An overview of the pedestrian-level VE and the total VE for various VCs is depicted in Fig. 8. The total VE varied from −4.0% to 20.6% while pedestrian-level VE from −3.5% to 15.4% depending on different VCs. The mean VEs of the total and the pedestrian-level were 5.0% and 5.2%, respectively. From all VCs comparisons, the best pedestrian-level VE (14.1% and 15.4%) and total VE (19.3% and 20.6%) were found by enhanced cases, especially by the case of $C_{Tree\ down\text{-}Shrub}$. For those only Tree used cases, the best VEs (pedestrian level: 3.3%–10.9%; total effect: 2.1%–11.5%) were found by leeward side planting, while the worst VEs (pedestrian level: −3.5%-4.8%; total effect: −4.0%-3.5%) were found by windward side planting. We also found that the VE of Cypress (pedestrian level: 4.8%–10.9%; total VE: 3.5%–11.5%) was better than the other two species for the same VC. Compared to Cypress on two sides ($C_{Cypress\text{-}Cypress}$), adding a row of shrub on the street axis between the Cypress ($C_{Tree\text{-}Shrub\text{-}Tree}$) significantly increased the total VE, however, decreased the pedestrian-level VE. In general, the role of vegetation in the street-canyon had a positive effect in most cases when considering deposition effect even under perpendicular wind direction.

3.3. Impact of vegetation parameters on the VE

In terms of deposition effect, VE highly depends on the leaf area density (LAD) and the deposition velocity (v_d). In terms of aerodynamic effect, VE depends on drag coefficient (C_d) and leaf area density (LAD). Therefore, the parameters $LADv_d$ and C_dLAD driving

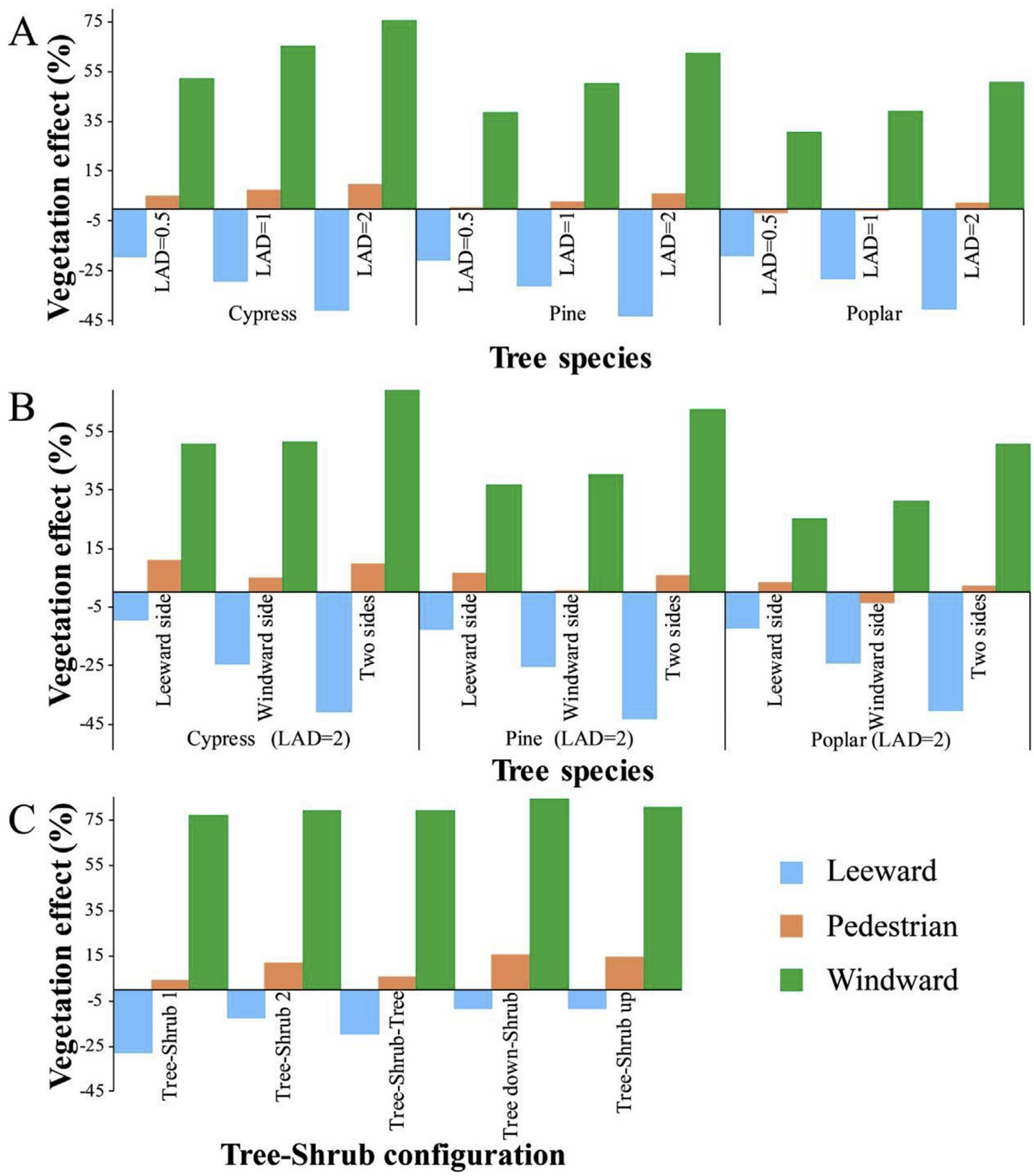

Fig. 7. VEs on the leeward wall, windward wall and pedestrian level of different tree species by (A) two sides planting, (B) one side planting and (C) Tree-Shrub configurations.

the VEs of two sides planting were analyzed.

3.3.1. Deposition parameter ($LADv_d$)

The VE against $LADv_d$ for the leeward wall was different from that for the windward wall and pedestrian level (Fig. 9A). The VE of leeward wall decreased as the $LADv_d$ increased. Conversely, VEs for windward wall and pedestrian level were significantly increased ($P < 0.001$) against the increase in $LADv_d$.

3.3.2. Aerodynamic parameter (C_dLAD)

Contrasting relationships of VEs and aerodynamic parameters (C_dLAD) were found between the leeward wall and pedestrian level/windward wall (Fig. 9B). The VE for the leeward wall was significantly decreased ($P < 0.001$) as the C_dLAD increase, while the VEs for both the windward wall and pedestrian level increased against the increase in C_dLAD.

4. Discussion

4.1. Leeward and windward

Fine particulate pollution levels near the building in the street-canyon is of great concern for indoor residents and workers (Karottki et al., 2015). For the perpendicular wind, two dominating flow phenomena in the street-canyon, a canyon vortex in the central part and corner eddies at the ends. The higher concentrations on the leeward wall than windward wall in the treeless street-canyon, which is mainly controlled by horizontally rotating canyon vortex (Gromke and Ruck, 2007). This vortex drives air from the building roof flow downward into the windward wall and then towards leeward wall (Gromke et al., 2016). As a result, the pollutants concentration on the windward wall is diluted and traffic pollutants were accumulated on the leeward wall. Moreover, the higher PM concentration were found in the street center than the street ends (Buccolieri et al., 2009). The canyon vortex is the only

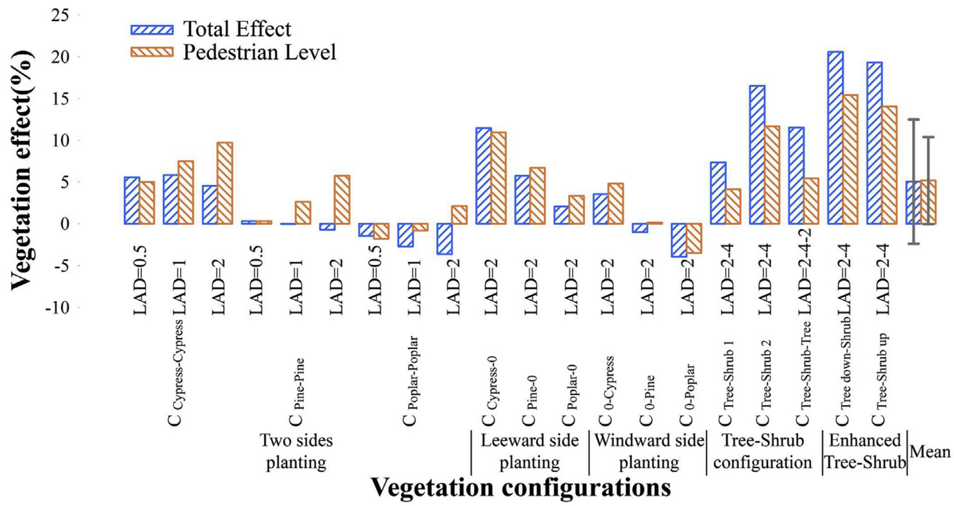

Fig. 8. The pedestrian-level VE and the total VE for all VCs.

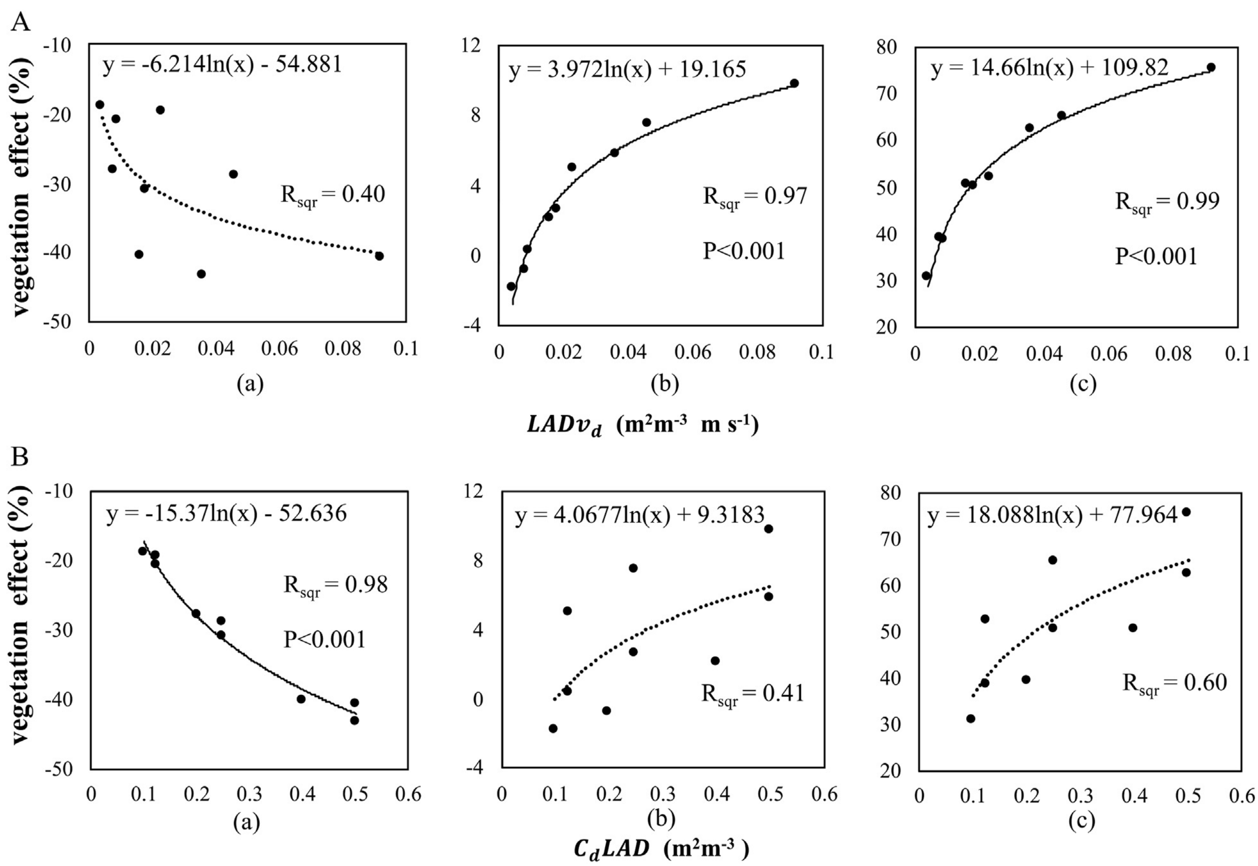

Fig. 9. Relationships between VE and vegetation parameters: Panel (A) represents deposition parameter ($LADv_d$) and panel (B) represents aerodynamic parameter (C_dLAD). In each panel, (a) leeward wall, (b) pedestrian level, and (c) windward wall.

source of air exchange for the canyon center part, while for the street ends, a better ventilation due to the superposition of both the canyon vortex and corner eddies (Gromke and Ruck, 2007). For the perpendicular wind, the introduction of vegetation into the street-canyon could increase the PM concentration near the leeward wall and reduce the PM concentration level near the windward (Buccolieri et al., 2018). Compared to treeless case, the lowest negative VEs (−8.3% and −8.5%) for the leeward wall were found in two enhanced cases. Vegetation act as flow obstacles that reduces the flow velocities, with the smaller flow velocities implying a reduced air volume flux in the canyon vortex (Gromke et al., 2008), so the pollutant was less diluted (Ji and Zhao, 2014).

4.2. Pedestrian level

Fine particulate pollution level at the breath-height of pedestrians in the street-canyon is a primary concern for the walkers and bikers (Karottki et al., 2015), as the fine particles can be easily breathed into pulmonary alveoli (Chen et al., 2016) resulting in more cardiovascular and respiratory diseases (Hofman et al., 2013). Compared to other VCs, $C_{Tree\text{-}Shrub2}$, $C_{Tree\ down\text{-}Shrub}$ and $C_{Tree\text{-}Shrub\ up}$ could make VE reach to 11.6–15.4% in pedestrian-level and 16.5–20.6% in total, respectively (Fig. 8). The reason may be the larger leaf area density, higher deposition velocity and closer distance to the source of traffic pollutant provided by the shrub. The sidewise shrub limited the lateral dispersion in the bottom part of the street canyon (Gromke et al., 2016), thus more traffic PM circulate between the vegetation and more particles are deposited. A planting design should consider this condition by providing as great a plant surface as possible near the emission source without significantly reducing air exchange (Litschke and Kuttler, 2008). As a result, the leeward side planting had a better VE than windward side planting and two sides planting, because the tree on the leeward side are closer to the higher polluted area compared to windward side planting under the perpendicular wind. At the same time, the obstructing effect of vegetation of leeward side planting is less reduced compared with two sides planting. Compared to $C_{Cypress\text{-}Cypress}$, the $C_{Tree\text{-}Shrub\text{-}Tree}$ significantly reduced the pedestrian-level VE because the shrub on the street axis hindered the pollutant dispersion of the pedestrian level, however, the total VE was improved due to more PM deposition. The planting position and the VC may be more critical than the volume of vegetation. Collectively, vegetation had a regionally beneficial impact on street air quality by 0.1%–15.4% at pedestrian level and 0.3%–20.6% in total, which is an important finding with regard to air quality issues in street-canyons (Jeanjean et al., 2015).

4.3. Impact of vegetation parameters on the VE

4.3.1. Deposition parameter ($LADv_d$)

Overall, the deposition effects are larger for increased *LAD* and v_d (Buccolieri et al., 2018). However, the larger *LAD* may also cause the aerodynamic effect for reducing the ventilation; the v_d may be the most important vegetation parameter for the selection roadside vegetation to improve air quality inside the street-canyon (Xue and Li, 2017). The range of dry deposition velocities in the literature is very wide, as dry deposition velocities are highly dependent on the vegetation species and particle sizes (Jeanjean et al., 2016). In this study, the Cypress VE was better than the other species for same VC (Fig. 8) due to high v_d of Cypress that can accumulate more particles on the leaves. For different VCs, the VE of $C_{Tree\text{-}Shrub\ 2}$ was better than that of $C_{Tree\text{-}Shrub\ 1}$ (Fig. 7C) due to a higher v_d for the shrub. The deposition amount and efficiency can be promoted by increased v_d, and the air quality in the street-canyon may be ultimately improved (Janhäll, 2015).

4.3.2. Aerodynamic parameter (C_dLAD)

The pressure loss coefficient (C_dLAD) ranging between 0.04 and 1.35 m^{-1} for common tree species (Xue and Li, 2017) is a critical aerodynamic parameter that affects airflow and pollutant transport. Poplar has less drag coefficient than Cypress and Pine. The wind permeability of Poplar canopy is larger than conifer canopy due to the difference in the flexibility of the leaves (Koizumi et al., 2010). In addition, there is a complex aerodynamic implication of vegetation canopy resistance. For example, aerodynamic effect of vegetation can decrease the wind velocity but increase the turbulence (Mochida et al., 2008). Trees can alter the flow pattern, turbulent exchange of mass, and consequently affect pollutant concentration (Buccolieri et al., 2011). For the perpendicular wind, the aerodynamic drag was unfavorable for the leeward wall but favorable for the windward wall. This is due to the drag force of vegetation that blocked the flow of air and pollutant transportation (Gromke and Ruck, 2012). Similarly, the impermeable screen covered with hedge effectively shield the footpath from the elevated traffic concentrations, leading to lower concentrations at the footpath with respect to the scenario without vegetation (Vos et al., 2013). The enhanced Tree-Shrub configurations could reduce negative VE of the leeward wall and mitigate highly concentrated pollution of the leeward and windward wall in the street center, because we were making good use of aerodynamic effect to change the flow field and alter pollutant distribution (Jeanjean et al., 2017). Therefore, the aerodynamic effect of roadside vegetation to change the flow field for reducing the pollutant level in a street-canyon can be significant.

5. Conclusions

This study investigated the aerodynamic and deposition effects of different vegetation configurations with several tree species on traffic-induced PM pollutant in a street-canyon. To do so, the study quantified the VEs for VCs and explored the governing mechanism of vegetation parameters on VEs. We concluded that vegetation can improve street-canyon air quality for the most investigated VCs under the perpendicular wind. More specifically, we found that an optimal VC strategy could reduce street-canyon traffic emissions by 20.6%. The VE can be promoted by making good use of the aerodynamic effect to alter pollutants distribution and selecting vegetation with a high deposition velocity to filter more pollutants. An optimized planting design may be more important than the volume of the vegetation in terms of PM reduction. The above-mentioned results could offer an effective guide for urban planners in vegetation planting design for the creation of a healthier urban environment.

CRediT authorship contribution statement

Lu Zhang: Conceptualization, Methodology, Investigation, Formal analysis, Visualization, Writing - original draft. **Zhiqiang Zhang:** Conceptualization, Methodology, Supervision, Writing - review & editing. **Steven McNulty:** Writing - review & editing. **Ping Wang:** Writing - review & editing.

Declaration of competing interest

The authors declare that they have no known competing financial interests or personal relationships that could have appeared to influence the work reported in this paper.

Acknowledgment

Authors greatly appreciate the financial support from the State Forestry and Grassland Administration of China through Forestry Public Welfare Research Project (Grant No. 20130430103) and Beijing Municipal Education Commission through Innovative Transdisciplinary Program "Ecological Restoration Engineering". We gratefully acknowledge the anonymous reviewers for their constructive and insightful comments and suggestions that helped us improve significantly the original version of this paper.

References

Abhijith, K.V., Kumar, P., Gallagher, J., Mcnabola, A., Baldauf, R., Pilla, F., Broderick, B., Di, S., Pulvirenti, B., 2017. Air pollution abatement performances of green infrastructure in open road and built-up street canyon environments - a review. Atmos. Environ. 162, 71–86. https://doi.org/10.1016/j.atmosenv.2017.05.014.

Al-Dabbous, A.N., Kumar, P., 2014. The influence of roadside vegetation barriers on airborne nanoparticles and pedestrians exposure under varying wind

conditions. Atmos. Environ. 90, 113–124. https://doi.org/10.1016/j.atmosenv.2014.03.040.
Beckett, K.P., Freer-smith, P.H., Taylor, G., 2000. Particulate pollution capture by urban trees: effect of species and windspeed. Global Change Biol. 6, 995–1003. https://doi.org/10.1046/j.1365-2486.2000.00376.x.
Blocken, B., Stathopoulos, T., Saathoff, P., Wang, X., 2008. Numerical evaluation of pollutant dispersion in the built environment: comparisons between models and experiments. J. Wind Eng. Ind. Aerod. 96, 1817–1831. https://doi.org/10.1016/j.jweia.2008.02.049.
Buccolieri, R., Gromke, C., Di Sabatino, S., Ruck, B., 2009. Aerodynamic effects of trees on pollutant concentration in street canyons. Sci. Total Environ. 407, 5247–5256. https://doi.org/10.1016/j.scitotenv.2009.06.016.
Buccolieri, R., Jeanjean, A.P.R., Gatto, E., Leigh, R.J., 2018. The impact of trees on street ventilation, NOx and PM2.5 concentrations across heights in Marylebone Rd street canyon, central London. Sustain. Cities Soc. 41, 227–241. https://doi.org/10.1016/j.scs.2018.05.030.
Buccolieri, R., Salim, S.M., Leo, L.S., Di Sabatino, S., Chan, A., Ielpo, P., de Gennaro, G., Gromke, C., 2011. Analysis of local scale tree-atmosphere interaction on pollutant concentration in idealized street canyons and application to a real urban junction. Atmos. Environ. 45, 1702–1713. https://doi.org/10.1016/j.atmosenv.2010.12.058.
Chen, C., Zhao, B., Zhou, W., Jiang, X., Tan, Z., 2012. A methodology for predicting particle penetration factor through cracks of windows and doors for actual engineering application. Build. Environ. 47, 339–348. https://doi.org/10.1016/j.buildenv.2011.07.004.
Chen, L., Liu, C., Zou, R., Yang, M., Zhang, Z., 2016. Experimental examination of effectiveness of vegetation as bio-filter of particulate matters in the urban environment. Environ. Pollut. 208, 198–208. https://doi.org/10.1016/j.envpol.2015.09.006.
Di Sabatino, S., Buccolieri, R., Pulvirenti, B., Britter, R.E., 2008. Flow and pollutant dispersion in street canyons using FLUENT and ADMS-Urban. Environ. Model. Assess. 13, 369–381. https://doi.org/10.1007/s10666-007-9106-6.
Dzierżanowski, K., Popek, R., Gawrońska, H., Sæbø, A., Gawroński, S.W., 2011. Deposition of particulate matter of different size fractions on leaf surfaces and in waxes of urban forest species. Int. J. Phytoremediation 13, 1037–1046. https://doi.org/10.1080/15226514.2011.552929.
Endalew, A.M., Hertog, M., Delele, M.A., Baetens, K., Persoons, T., Baelmans, M., Ramon, H., Nicolaï, B.M., Verboven, P., 2009. CFD modelling and wind tunnel validation of airflow through plant canopies using 3D canopy architecture. Int. J. Heat Fluid Flow 30, 356–368. https://doi.org/10.1016/j.ijheatfluidflow.2008.12.007.
Freer-smith, P.H., Beckett, K.P., Taylor, G., 2005. Deposition velocities to Sorbus aria , Acer campestre , Populus deltoides × trichocarpa 'Beaupré', Pinus nigra and × Cupressocyparis leylandii for coarse, fine and ultra-fine particles in the urban environment. Environ. Pollut. 133, 157–167. https://doi.org/10.1016/j.envpol.2004.03.031.
Gousseau, P., Blocken, B., van Heijst, G.J.F., 2011. CFD simulation of pollutant dispersion around isolated buildings: on the role of convective and turbulent mass fluxes in the prediction accuracy. J. Hazard Mater. 194, 422–434. https://doi.org/10.1016/j.jhazmat.2011.08.008.
Gromke, C., 2013. CODASC: a database for the validation of street canyon dispersion models. In: The 15th International Conference on Harmonisation within Atmospheric Dispersion Modelling for Regulatory Purposes (HARMO).
Gromke, C., 2011. A vegetation modeling concept for building and environmental aerodynamics wind tunnel tests and its application in pollutant dispersion studies. Environ. Pollut. 159, 2094–2099. https://doi.org/10.1016/j.envpol.2010.11.012.
Gromke, C., Blocken, B., 2015. Influence of avenue-trees on air quality at the urban neighborhood scale. Part I: quality assurance studies and turbulent Schmidt number analysis for RANS CFD simulations. Environ. Pollut. 196, 214–223. https://doi.org/10.1016/j.envpol.2014.10.016.
Gromke, C., Buccolieri, R., Di Sabatino, S., Ruck, B., 2008. Dispersion study in a street canyon with tree planting by means of wind tunnel and numerical investigations - evaluation of CFD data with experimental data. Atmos. Environ. 42, 8640–8650. https://doi.org/10.1016/j.atmosenv.2008.08.019.
Gromke, C., Jamarkattel, N., Ruck, B., 2016. Influence of roadside hedgerows on air quality in urban street canyons. Atmos. Environ. 139, 75–86. https://doi.org/10.1016/j.atmosenv.2016.05.014.
Gromke, C., Ruck, B., 2012. Pollutant concentrations in street canyons of different aspect ratio with avenues of trees for various wind directions. Boundary-Layer Meteorol. 144, 41–64. https://doi.org/10.1007/s10546-012-9703-z.
Gromke, C., Ruck, B., 2009. On the impact of trees on dispersion processes of traffic emissions in street canyons. Boundary-Layer Meteorol. 131, 19–34. https://doi.org/10.1007/s10546-008-9301-2.
Gromke, C., Ruck, B., 2007. Influence of trees on the dispersion of pollutants in an urban street canyon-Experimental investigation of the flow and concentration field. Atmos. Environ. 41, 3287–3302. https://doi.org/10.1016/j.atmosenv.2006.12.043.
Haakman, R., Beenakker, I., Geerlings, H., 2020. Reducing vehicle-related NOx and PM emissions in metropolitan areas: a comparison between the Randstad and the Rhine-Ruhr area. J. Clean. Prod. 247, 119175 https://doi.org/10.1016/j.jclepro.2019.119175.
Hanna, S., Chang, J., 2012. Acceptance criteria for urban dispersion model evaluation. Meteorol. Atmos. Phys. 116, 133–146. https://doi.org/10.1007/s00703-011-0177-1.
Hofman, J., Bartholomeus, H., Janssen, S., Calders, K., Wuyts, K., Van Wittenberghe, S., Samson, R., 2016. Influence of tree crown characteristics on the local PM 10 distribution inside an urban street canyon in Antwerp (Belgium): a model and experimental approach. Urban For. Urban Green. 20, 265–276. https://doi.org/10.1016/j.ufug.2016.09.013.
Hofman, J., Stokkaer, I., Snauwaert, L., Samson, R., 2013. Spatial distribution assessment of particulate matter in an urban street canyon using biomagnetic leaf monitoring of tree crown deposited particles. Environ. Pollut. 183, 123–132. https://doi.org/10.1016/j.envpol.2012.09.015.
Hong, B., Lin, B., Qin, H., 2017. Numerical investigation on the coupled e ff ects of building-tree arrangements on fi ne particulate matter (PM 2.5) dispersion in housing blocks. Sustain. Cities Soc. 34, 358–370. https://doi.org/10.1016/j.scs.2017.07.005.
Janhäll, S., 2015. Review on urban vegetation and particle air pollution- Deposition and dispersion. Atmos. Environ. 105, 130–137. https://doi.org/10.1016/j.atmosenv.2015.01.052.
Jeanjean, A.P.R., Buccolieri, R., Eddy, J., Monks, P.S., Leigh, R.J., 2017. Air quality affected by trees in real street canyons : the case of Marylebone neighbourhood in central London. Urban For. Urban Green. 22, 41–53. https://doi.org/10.1016/j.ufug.2017.01.009.
Jeanjean, A.P.R., Hinchliffe, G., McMullan, W.A., Monks, P.S., Leigh, R.J., 2015. A CFD study on the effectiveness of trees to disperse road traffic emissions at a city scale. Atmos. Environ. 120, 1–14. https://doi.org/10.1016/j.atmosenv.2015.08.003.
Jeanjean, A.P.R., Monks, P.S., Leigh, R.J., 2016. Modelling the effectiveness of urban trees and grass on PM 2.5 reduction via dispersion and deposition at a city scale. Atmos. Environ. 147, 1–10. https://doi.org/10.1016/j.atmosenv.2016.09.033.
Ji, W., Zhao, B., 2015. Estimating mortality derived from indoor exposure to particles of outdoor origin. PloS One 10, 1–15. https://doi.org/10.1371/journal.pone.0124238.
Ji, W., Zhao, B., 2014. Numerical study of the effects of trees on outdoor particle concentration distributions. Build. Simul. 7, 417–427. https://doi.org/10.1007/s12273-014-0180-9.
Jin, S., Guo, J., Wheeler, S., Kan, L., Che, S., 2014. Evaluation of impacts of trees on PM2.5 dispersion in urban streets. Atmos. Environ. 99, 277–287. https://doi.org/10.1016/j.atmosenv.2014.10.002.
Karottki, D.G., Spilak, M., Frederiksen, M., Andersen, Z.J., Madsen, A.M., Ketzel, M., Massling, A., Gunnarsen, L., Møller, P., Loft, S., 2015. Indoor and outdoor exposure to ultrafine, fine and microbiologically derived particulate matter related to cardiovascular and respiratory effects in a panel of elderly urban citizens. Int. J. Environ. Res. Publ. Health 12, 1667–1686. https://doi.org/10.3390/ijerph120201667.
Katul, G.G., Mahrt, L., Poggi, D., Sanz, C., 2004. One- and two-equation models for canopy turbulence. Boundary-Layer Meteorol. 113, 81–109. https://doi.org/10.1023/B:BOUN.0000037333.48760.e5.
Koizumi, A., Motoyama, J. ichi, Sawata, K., Sasaki, Y., Hirai, T., 2010. Evaluation of drag coefficients of poplar-tree crowns by a field test method. J. Wood Sci. 56, 189–193. https://doi.org/10.1007/s10086-009-1091-8.
Kumar, P., Fennell, P., Britter, R., 2008. Effect of wind direction and speed on the dispersion of nucleation and accumulation mode particles in an urban street canyon. Sci. Total Environ. 402, 82–94. https://doi.org/10.1016/j.scitotenv.2008.04.032.
Lelieveld, J., Evans, J.S., Fnais, M., Giannadaki, D., Pozzer, A., 2015. The contribution of outdoor air pollution sources to premature mortality on a global scale. Nature 525, 367–371. https://doi.org/10.1038/nature15371.
Litschke, T., Kuttler, W., 2008. On the reduction of urban particle concentration by vegetation - a review. Meteorol. Z. 17, 229–240. https://doi.org/10.1127/0941-2948/2008/0284.
Liu, S., Pan, W., Zhang, H., Cheng, X., Long, Z., Chen, Q., 2017. CFD simulations of wind distribution in an urban community with a full-scale geometrical model. Build. Environ. 117, 11–23. https://doi.org/10.1016/j.buildenv.2017.02.021.
Mitchell, R., Maher, B.A., Kinnersley, R., 2010. Rates of particulate pollution deposition onto leaf surfaces: temporal and inter-species magnetic analyses. Environ. Pollut. 158, 1472–1478. https://doi.org/10.1016/j.envpol.2009.12.029.
Mochida, A., Tabata, Y., Iwata, T., Yoshino, H., 2008. Examining tree canopy models for CFD prediction of wind environment at pedestrian level. Wind Eng. Ind. Aerodyn. 96, 1667–1677. https://doi.org/10.1016/j.jweia.2008.02.055.
Qin, H., Hong, B., Jiang, R., Yan, S., Zhou, Y., 2019. The effect of vegetation enhancement on particulate pollution reduction: CFD simulations in an urban park. Forests 10, 373. https://doi.org/10.3390/f10050373.
Salim, S.M., Buccolieri, R., Chan, A., Di Sabatino, S., 2011. Numerical simulation of atmospheric pollutant dispersion in an urban street canyon: comparison between RANS and LES. J. Wind Eng. Ind. Aerod. 99, 103–113. https://doi.org/10.1016/j.jweia.2010.12.002.
Salmond, J.A., Williams, D.E., Laing, G., Kingham, S., Dirks, K., Longley, I., Henshaw, G.S., 2013. The influence of vegetation on the horizontal and vertical distribution of pollutants in a street canyon. Sci. Total Environ. 443, 287–298. https://doi.org/10.1016/j.scitotenv.2012.10.101.
Sanz, C., 2003. A NOTE ON $k - \varepsilon$ MODELLING OF VEGETATION CANOPY AIR-FLOWS research note. Boundary-Layer Meteorol. 108, 191–197.
Song, Y., Wang, X., Maher, B.A., Li, F., Xu, C., Liu, X., Sun, X., Zhang, Z., 2016. The spatial-temporal characteristics and health impacts of ambient fine particulate matter in China. J. Clean. Prod. 112, 1312–1318. https://doi.org/10.1016/j.jclepro.2015.05.006.
Terzaghi, E., Wild, E., Zacchello, G., Cerabolini, B.E.L., Jones, K.C., Di Guardo, A., 2013. Forest filter effect: role of leaves in capturing/releasing air particulate matter and its associated PAHs. Atmos. Environ. 74, 378–384. https://doi.org/10.1016/j.atmosenv.2013.04.013.
Toparlar, Y., Blocken, B., Maiheu, B., van Heijst, G.J.F., 2017. A review on the CFD analysis of urban microclimate. Renew. Sustain. Energy Rev. 80, 1613–1640.

https://doi.org/10.1016/j.rser.2017.05.248.

Vos, P.E.J., Maiheu, B., Vankerkom, J., Janssen, S., 2013. Improving local air quality in cities : to tree or not to tree ? Environ. Pollut. 183, 113–122. https://doi.org/10.1016/j.envpol.2012.10.021.

Vranckx, S., Vos, P., Maiheu, B., Janssen, S., 2015. Impact of trees on pollutant dispersion in street canyons: a numerical study of the annual average effects in Antwerp, Belgium. Sci. Total Environ. 532, 474–483. https://doi.org/10.1016/j.scitotenv.2015.06.032.

Wu, J., Zheng, H., Zhe, F., Xie, W., Song, J., 2018. Study on the relationship between urbanization and fine particulate matter (PM2.5) concentration and its implication in China. J. Clean. Prod. 182, 872–882. https://doi.org/10.1016/j.jclepro.2018.02.060.

Xue, F., Li, X., 2017. The impact of roadside trees on traffic released PM 10 in urban street canyon : aerodynamic and deposition effects. Sustain. Cities Soc. 30, 195–204. https://doi.org/10.1016/j.scs.2017.02.001.

Yang, H., Chen, T., Lin, Y., Buccolieri, R., Mattsson, M., Zhang, M., Hang, J., Wang, Q., 2020. Integrated impacts of tree planting and street aspect ratios on CO dispersion and personal exposure in full-scale street canyons. Build. Environ. 169, 106529 https://doi.org/10.1016/j.buildenv.2019.106529.